Polarization of Λ and Λ̄ Hyperons along the Beam Direction in Pb-Pb Collisions at √sNN = 5.02 TeV

(ALICE Collaboration) Acharya, S.; ...; Erhardt, Filip; ...; Gotovac, Sven; ...; Jerčić, Marko; ...; Karatović, David; ...; ...

Source / Izvornik: **Physical Review Letters, 2022, 128**

Journal article, Published version
Rad u časopisu, Objavljena verzija rada (izdavačev PDF)

https://doi.org/10.1103/PhysRevLett.128.172005

Permanent link / Trajna poveznica: https://urn.nsk.hr/urn:nbn:hr:217:434962

Polarization of Λ and $\bar{\Lambda}$ Hyperons along the Beam Direction in Pb-Pb Collisions at $\sqrt{s_{NN}} = 5.02$ TeV

S. Acharya *et al.*[*]
(ALICE Collaboration)

(Received 3 September 2021; revised 4 January 2022; accepted 16 March 2022; published 29 April 2022)

The polarization of the Λ and $\bar{\Lambda}$ hyperons along the beam (z) direction, P_z, has been measured in Pb-Pb collisions at $\sqrt{s_{NN}} = 5.02$ TeV recorded with ALICE at the Large Hadron Collider (LHC). The main contribution to P_z comes from elliptic flow-induced vorticity and can be characterized by the second Fourier sine coefficient $P_{z,s2} = \langle P_z \sin(2\varphi - 2\Psi_2)\rangle$, where φ is the hyperon azimuthal emission angle and Ψ_2 is the elliptic flow plane angle. We report the measurement of $P_{z,s2}$ for different collision centralities and in the 30%–50% centrality interval as a function of the hyperon transverse momentum and rapidity. The $P_{z,s2}$ is positive similarly as measured by the STAR Collaboration in Au-Au collisions at $\sqrt{s_{NN}} = 200$ GeV, with somewhat smaller amplitude in the semicentral collisions. This is the first experimental evidence of a nonzero hyperon P_z in Pb-Pb collisions at the LHC. The comparison of the measured $P_{z,s2}$ with the hydrodynamic model calculations shows sensitivity to the competing contributions from thermal and the recently found shear-induced vorticity, as well as to whether the polarization is acquired at the quark-gluon plasma or the hadronic phase.

DOI: 10.1103/PhysRevLett.128.172005

The system created in high-energy nuclear collisions behaves almost like an ideal fluid [1]. Its evolution is characterized by nontrivial velocity and vorticity fields, resulting in the polarization of the produced particles. In particular, the shear in the initial velocity distributions of the participants in off-center nuclear collisions leads to a nonzero vorticity component and a net particle polarization along the orbital momentum of the colliding nuclei, a phenomenon termed as global polarization [2–4]. Recent measurements at RHIC show a significant global polarization of Λ and $\bar{\Lambda}$ hyperons in Au-Au collisions at $\sqrt{s_{NN}} =$ 7.7–200 GeV with the polarization magnitude of a few to a fraction of a percent, monotonically decreasing with increasing $\sqrt{s_{NN}}$ [5,6]. The global hyperon polarization measured by the ALICE Collaboration in Pb-Pb collisions at $\sqrt{s_{NN}} = 2.76$ and 5.02 TeV [7] was found to be at the per mil level, consistent with zero within experimental uncertainties. The ALICE measurements are also consistent with hydrodynamical model calculations for the LHC energies and empirical estimates based on the collision energy dependence of the directed flow due to the tilted source [4,8,9]. The decrease in the global polarization at midrapidity with collision energy is usually attributed to a decreasing role of the baryon stopping [10] in the initial velocity distributions.

In addition to the vorticity due to the orbital angular momentum of the entire system, other physics processes, such as anisotropic flow, jet energy deposition, and deviation from longitudinal boost invariance of the transverse velocity fields, generate vorticity [8,11–15] along different directions depending on the location of the fluid elements in the created system. It was predicted that, in noncentral nucleus-nucleus collisions, the strong elliptic flow would generate a nonzero vorticity component along the beam axis (z) [8,12]. The vorticity and the corresponding polarization exhibits a quadrupole structure in the transverse plane. This polarization, characterized by the second harmonic sine component in the Fourier decomposition of the polarization along the beam axis (P_z) as a function of the particle azimuthal angle (φ) relative to the elliptic flow plane Ψ_2, is evaluated as

$$P_{z,s2} = \langle P_z \sin(2\varphi - 2\Psi_2)\rangle. \quad (1)$$

The sign of $P_{z,s2}$ determines the phase of the P_z modulation in azimuth relative to the elliptic flow plane.

The Λ and $\bar{\Lambda}$ polarization along the beam direction was measured by the STAR Collaboration in Au-Au collisions at $\sqrt{s_{NN}} = 200$ GeV [16] and compared with the hydrodynamic [12], transport (AMPT) [14,17], and blast-wave (BW) [8,16] model calculations. The measured $P_{z,s2}$ was found to be about 5 times smaller in magnitude and of

[*]Full author list given at the end of the article.

opposite sign compared to the hydrodynamic and AMPT model predictions. However, the BW model, tuned to spectra, elliptic flow, and azimuthally differential femtoscopic measurements, describes the magnitude and the sign of $P_{z,s2}$. Most model calculations estimate the particle polarization from the thermal vorticity [12,17] at the freeze-out surface assuming local thermodynamic equilibrium of the spin degrees of freedom. Unlike hydrodynamic and AMPT calculations, the BW model [8,16] accounts only for the kinematic vorticity associated with the velocity fields without contribution from the temperature gradients and acceleration. It was confirmed by other calculations that the kinematic vorticity alone describes the RHIC results much better than the thermal vorticity [18]. In addition, the chiral kinetic approach with AMPT initial conditions [15], accounting for the transverse vorticity fields due to deviation from longitudinal boost invariance, generates the correct sign for $P_{z,s2}$. The difference in the sign of $P_{z,s2}$ between the experimental data and model calculations based on solely thermal vorticity has been a subject of intense investigations [14,15,17–19].

Recently, a possible explanation to the experimentally observed positive $P_{z,s2}$ at RHIC was proposed based on the additional contribution to polarization from fluid shear [20,21]. The studies in Refs. [22,23] demonstrate that the fluid shear competes with thermal vorticity and contributes with an opposite phase to the azimuthal angle dependence of hyperon spin polarization. Under the assumptions of isothermal (at constant temperature) hadronization or that the hyperons inherit the spin polarization of the constituent strange quark, the effect of shear prevails over thermal vorticity and their combined effect qualitatively explains the experimentally observed azimuthal angle dependence of the hyperon spin polarization in Au-Au collisions at $\sqrt{s_{NN}} = 200$ GeV [22,23]. These studies indicate that the longitudinal polarization is very sensitive to the hydrodynamic gradients and the evolution of the spin degrees of freedom through different stages of the evolution of the system created in heavy-ion collisions. The measurement of $P_{z,s2}$ in Pb-Pb collisions at $\sqrt{s_{NN}} = 5.02$ TeV and its comparison with measurements at RHIC as well as theoretical models can provide important insights into the fluid and spin dynamics in heavy-ion collisions.

In this Letter, we report the centrality, transverse momentum (p_T), and rapidity (y_H) dependences of $P_{z,s2}$ for Λ ($\bar{\Lambda}$) hyperons measured by the ALICE Collaboration in Pb-Pb collisions at $\sqrt{s_{NN}} = 5.02$ TeV and compare with the previous STAR measurements in Au-Au collisions at $\sqrt{s_{NN}} = 200$ GeV as well as with shear- and vorticity-based hydrodynamic model calculations for Pb-Pb collisions at $\sqrt{s_{NN}} = 5.02$ TeV.

As the spin of a particle cannot be measured directly, the parity-violating weak decays of $\Lambda \to p + \pi^-$ and $\bar{\Lambda} \to \bar{p} + \pi^+$, in which the momentum of the daughter (anti)proton is correlated with the spin of the hyperon, are used to measure the polarization. The angular distribution of the (anti)proton in the hyperon rest frame is given by [24]

$$4\pi \frac{dN}{d\Omega^*} = 1 + \alpha_H \mathbf{P}_H \cdot \hat{\mathbf{p}}_p^* = 1 + \alpha_H P_H \cos\theta_p^*, \quad (2)$$

where $\mathbf{P}_H$ is the polarization vector, α_H is the hyperon decay parameter ($\alpha_\Lambda = 0.750 \pm 0.009, \alpha_{\bar{\Lambda}} = -0.758 \pm 0.01$ [25]), $\hat{\mathbf{p}}_p^*$ is the unit vector along the (anti)proton momentum in the hyperon rest frame, and θ_p^* is the angle between the (anti)proton momentum and the polarization vector in the hyperon rest frame. To measure the polarization component along the z direction, θ_p^* is considered as the polar angle of the (anti)proton momentum in the hyperon rest frame. The polarization P_z can be estimated by averaging $\cos\theta_p^*$ over all hyperons in all collisions [16]:

$$P_z(p_T, y_H, \varphi) = \frac{\langle \cos\theta_p^* \rangle}{\alpha_H \langle (\cos\theta_p^*)^2 \rangle}, \quad (3)$$

where p_T, y_H, and φ are the transverse momentum, rapidity, and azimuthal angle of the hyperon, respectively. The factor $\langle (\cos\theta_p^*)^2 \rangle$, which equals to $1/3$ in the case of an ideal detector, is calculated directly from the data as a function of centrality, p_T, and y_H and serves as a correction for finite acceptance along the longitudinal direction.

The data used in this analysis were collected by ALICE [26,27] at the LHC in 2018 for Pb-Pb collisions at $\sqrt{s_{NN}} = 5.02$ TeV. Two datasets, corresponding to positive and negative magnetic field polarities, are considered for this measurement. The centrality is determined using the sum of the charge deposited in the V0A ($2.8 < \eta < 5.1$) and the V0C ($-3.7 < \eta < -1.7$) scintillator arrays, denoted as the V0M centrality [28]. The event selection is based on the trigger criteria and quality of the event vertex reconstruction using the Time Projection Chamber (TPC) [29] and the Inner Tracking System (ITS) [30]. Events that pass central, semicentral, or minimum-bias trigger criteria with a z component of the reconstructed event vertex (V_z) within ± 10 cm are selected. To suppress the pile-up of multiple collisions in the TPC drift volume, events with a TPC multiplicity beyond 5 times the width of its distribution at any V0M centrality are rejected. A similar cut on the ITS centrality for the corresponding V0M centrality is applied to get rid of additional outliers in the sample. In total, about 270M events are selected for the polarization measurement. The centrality dependence of $P_{z,s2}$ is studied with 10% centrality intervals, whereas the p_T and y_H dependence is studied in the semicentral (30%–50%) collisions where elliptic flow is the largest.

The Λ and $\bar{\Lambda}$ hyperons are reconstructed inside the TPC using the decay topology of $\Lambda \to p + \pi^-$ and $\bar{\Lambda} \to \bar{p} + \pi^+$ (64% branching ratio) [31] as described in Refs. [27,32]. The daughter tracks are assigned the identity of a pion or a (anti)proton based on the charge and particle identification using the specific energy loss (dE/dx) measurement in the

TPC. The tracks of the daughter pions and (anti)protons are selected within the pseudorapidity range of $|\eta| < 0.8$ inside the TPC. Topological cuts such as distance of closest approach (DCA) of the Λ and $\bar{\Lambda}$ candidates to the primary vertex (< 1.5 cm), DCA of the daughter tracks to the primary vertex (> 0.05 cm), DCA between the daughter tracks (< 0.5 cm), and cosine of the pointing angle, which is the angle between the momentum direction of the hyperon and the direction from the primary vertex to the decay point (> 0.997), are used to reduce the combinatorial background contribution to the invariant mass spectrum. The Λ and $\bar{\Lambda}$ candidates having $1.103 < M_{\rm inv} < 1.129$ GeV/c^2 with $p_T > 0.5$ GeV/c and $|y_H| < 0.5$ are considered in this measurement.

The event-plane method is used for the polarization measurement [33]. The second harmonic event plane is reconstructed using the TPC tracks and signals in the V0A and V0C scintillators. The X_2 and Y_2 components of the second harmonic flow vector are given by

$$X_2 = \frac{\sum_i w_i \cos(2\varphi_i)}{\sum w_i}, \qquad Y_2 = \frac{\sum_i w_i \sin(2\varphi_i)}{\sum w_i}, \quad (4)$$

where, in the case of the TPC, $w_i = 1$, φ_i is the azimuthal angle of track i, and the sum runs over all the tracks used in the flow vector construction. In the case of V0A and V0C, which consist of four concentric rings with each ring divided into eight segments, φ_i is the azimuthal angle of the center of the ith segment and w_i is the measured signal proportional to the number of particles detected in that segment.

The TPC flow vectors are reconstructed using tracks in the positive ($0.1 < \eta < 0.8$) and negative ($-0.8 < \eta < -0.1$) pseudorapidity regions and transverse momentum within $0.2 < p_T < 3.0$ GeV/c. The flow vector for the V0A or the V0C is constructed by averaging the flow vectors of four rings using the energy deposited in each ring as a weight. Because of the imperfect detector acceptance, varying beam conditions, the averages $\langle X_2 \rangle$ and $\langle Y_2 \rangle$ might deviate from zero. To compensate these variations, flow vectors are recentered [33] run by run as a function of the event centrality, event vertex position (V_x, V_y, V_z), and the time the event was taken during the run:

$$X_2' = X_2 - \langle X_2 \rangle, \qquad Y_2' = Y_2 - \langle Y_2 \rangle. \quad (5)$$

The second harmonic event-plane angle ($\Psi_2^{\rm EP}$) is constructed from the recentered flow vector components as

$$\Psi_2^{\rm EP} = \frac{1}{2}\tan^{-1}(Y_2'/X_2'). \quad (6)$$

The $P_{z,s2}$ is experimentally measured using $\Psi_2^{\rm EP}$ via

$$P_{z,s2} = \frac{\langle P_z \sin(2\varphi - 2\Psi_2^{\rm EP}) \rangle}{R(\Psi_2^{\rm EP})}, \quad (7)$$

where φ is the azimuthal emission angle of the particle and $\Psi_2^{\rm EP}$ is the reconstructed second harmonic event-plane angle. The $R(\Psi_2^{\rm EP})$ is the event-plane resolution correction [33]. The $P_{z,s2}$ is estimated using the invariant mass method [16] by calculating $Q = \langle \cos\theta_p^* \sin(2\varphi - 2\Psi_2^{\rm EP}) \rangle$ for all hyperon candidates as a function of the invariant mass and fitting it with the expression

$$Q(M_{\rm inv}) = f^S(M_{\rm inv}) Q^S + f^{\rm BG} Q^{\rm BG}(M_{\rm inv}), \quad (8)$$

where f^S and $f^{\rm BG} = 1 - f^S$ are the signal and background fraction, respectively, of the Λ and $\bar{\Lambda}$ candidates estimated from the invariant mass yields. The constant Q^S estimates the signal, and $Q^{\rm BG}(M_{\rm inv})$ estimates the possible contribution from the combinatorial background of Λ and $\bar{\Lambda}$ hyperons toward the measured polarization. By default, the results are obtained using the assumption of zero background contribution [$Q^{\rm BG}(M_{\rm inv}) = 0$] to the hyperon polarization. The results obtained with the assumption of $Q^{\rm BG}(M_{\rm inv})$ being a linear function of $M_{\rm inv}$ are found to be consistent with the default case indicating the measured polarization is not sensitive to this assumption. Figure 1 shows an example of the fit to the invariant mass dependence of $Q(M_{\rm inv})$ using Eq. (8) for $\bar{\Lambda}$ in the 30%–40% centrality class. The $P_{z,s2}$ is obtained from Q^S after accounting for the finite detector acceptance [$\langle(\cos\theta_p^*)^2\rangle$], event-plane resolution correction, and scaling it with the hyperon decay constant (α_H).

The correction for the resolution of the second-order event planes reconstructed in the TPC, V0A, and V0C detectors are estimated using the three-subevent method with the set of [TPC, V0A, V0C] and [V0, TPC-left ($-0.8 < \eta < -0.1$), TPC-right ($0.1 < \eta < 0.8$)] event planes [33]. For midcentral collisions, the event-plane resolution correction peaks at ~0.88 for the TPC and

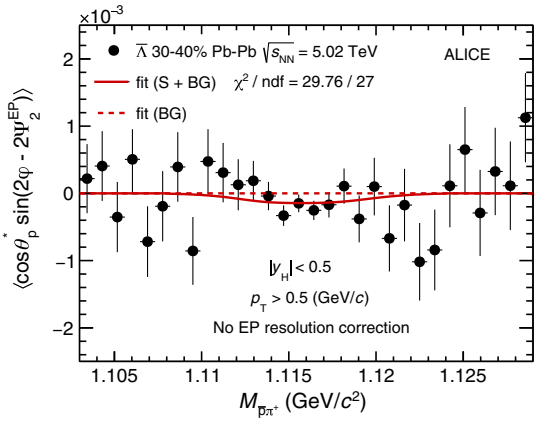

FIG. 1. Fit to the invariant mass dependence of the $\langle \cos\theta_p^* \sin(2\varphi - 2\Psi_2^{\rm EP}) \rangle$ for $\bar{\Lambda}$ before event-plane resolution correction using Eq. (8) in the 30%–40% centrality class. See the text for details.

~0.84 for the combined V0A and V0C detectors. The results obtained using the event planes reconstructed in the TPC and V0 detectors are found to be consistent with each other and are combined to reduce the statistical uncertainty considering the correlations between the event planes reconstructed in two detectors. The $P_{z,s2}$ measured for Λ and $\bar{\Lambda}$ hyperons are consistent with each other as expected for the polarization due to the elliptic flow-induced vorticity and combined to calculate the average hyperon polarization along the beam direction. A large fraction of the measured Λ and $\bar{\Lambda}$ hyperons originate from the decay of heavier resonances. In Ref. [34], it was shown that, under the assumption of similar vorticity-induced polarization for all final-state particles, the effect of feed-down is small, of the order of 15%. Similar to the previous STAR measurement [16], this measurement is not corrected for this effect.

The systematic uncertainties of this measurement are evaluated by varying the criteria for the selection of the events, hyperon daughters and topology of the decay, assumptions on the possible contributions from the Λ and $\bar{\Lambda}$ background toward the measured polarization, the p_T-dependent reconstruction efficiency, and comparing results obtained with different magnetic field orientations. The efficiency is estimated from a Monte Carlo event generator HIJING [35] by transporting the generated particles through GEANT3 [36] simulated detector response and performing track reconstruction in the ALICE reconstruction framework. The effect of the efficiency dependence on the hyperon transverse momentum is found to be negligible. The differences between the results estimated with the default and varied parameters, if found statistically significant from the Barlow criterion [37], are considered as a source of systematic uncertainty. The Barlow criterion is applied for each interval of centrality, p_T, and y_H for which the final polarization results are presented. If the Barlow criterion passes for more than 25% of the total intervals, the contribution of that particular systematic source is included in the measurement uncertainty. The contributions from the different sources are added in quadrature to estimate the total systematic uncertainty.

The centrality, p_T, and y_H dependences of $P_{z,s2}$ in Pb-Pb collisions at $\sqrt{s_{NN}} = 5.02$ TeV are shown in Figs. 2–4. The $P_{z,s2}$ decreases toward more central collisions, similar to the elliptic flow. For centralities larger than 60%, the large uncertainties prevent a firm conclusion on its centrality dependence. The $P_{z,s2}$ also shows an increase with p_T up to $p_T \approx 2.0$ GeV/c in the 30%–50% centrality interval. For higher p_T ($p_T > 2.0$ GeV/c), the $P_{z,s2}$ is consistent with being constant, but the uncertainty in the measurement does not allow for a strong conclusion. The ALICE results are compared with the STAR measurements in Au-Au collisions at $\sqrt{s_{NN}} = 200$ GeV [16] in Figs. 2 and 3. As the STAR results were obtained with $\alpha_H = 0.642$ whereas the ALICE measurement uses updated values $\alpha_H = 0.750$ (Λ) and -0.758 ($\bar{\Lambda}$), the STAR results are rescaled with a factor

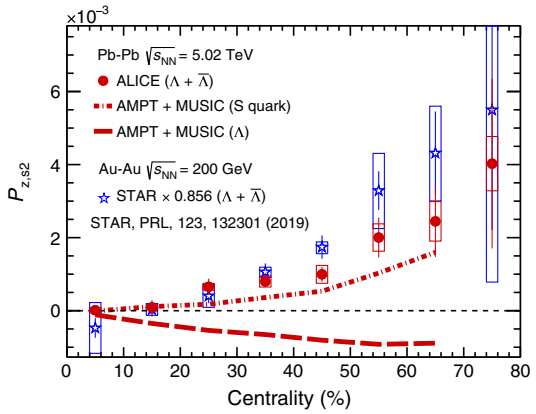

FIG. 2. Centrality dependence of $P_{z,s2}$ averaged for Λ and $\bar{\Lambda}$ in Pb-Pb collisions at $\sqrt{s_{NN}} = 5.02$ TeV and its comparison with the RHIC results for Au-Au collisions at $\sqrt{s_{NN}} = 200$ GeV. The model calculations [38] for Λ and strange quark for Pb-Pb collisions at $\sqrt{s_{NN}} = 5.02$ TeV using the approach described in Ref. [23] are shown by dash-dotted lines.

0.856 for a proper comparison. Figure 2 indicates that the hyperon polarization in Pb-Pb collisions at $\sqrt{s_{NN}} = 5.02$ TeV is similar in magnitude for the central collisions with somewhat smaller value in the semicentral collisions compared to the top RHIC energy. The latter seems to originate at lower transverse momenta ($p_T < 2.0$ GeV/c), where $P_{z,s2}$ at the LHC is smaller than that at the top RHIC energy in semicentral collisions as shown in Fig. 3. The $P_{z,s2}$ does not exhibit a significant dependence on rapidity as shown in Fig. 4.

The comparison between the ALICE results and the $P_{z,s2}$ values estimated from the fluid shear and thermal vorticity in a hydrodynamic model following the scheme used in

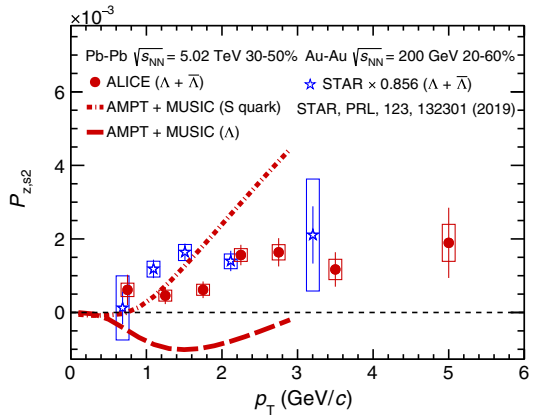

FIG. 3. Transverse momentum dependence of $P_{z,s2}$ averaged for Λ and $\bar{\Lambda}$ in Pb-Pb collisions at $\sqrt{s_{NN}} = 5.02$ TeV in semicentral collisions and its comparison with the similar RHIC results for Au-Au collisions at $\sqrt{s_{NN}} = 200$ GeV. The model calculations [38] for Λ and strange quark for Pb-Pb collisions at $\sqrt{s_{NN}} = 5.02$ TeV in the 30%–50% centrality interval using the approach described in Ref. [23] are shown by dash-dotted lines.

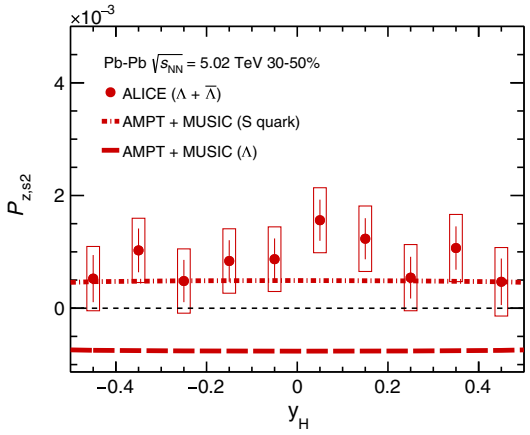

FIG. 4. The rapidity dependence of $P_{z,s2}$ averaged for Λ and $\bar{\Lambda}$ in Pb-Pb collisions at $\sqrt{s_{NN}} = 5.02$ TeV in semicentral collisions. The model calculations [38] for Λ and strange quark for Pb-Pb collisions at $\sqrt{s_{NN}} = 5.02$ in the 30%–50% centrality interval using the approach described in Ref. [23] are shown by dash-dotted lines.

Ref. [23] is shown in Figs. 2–4. The $3+1$ D hydrodynamical model MUSIC [39,40] with AMPT initial conditions [41,42], tuned to describe the $dN_{\rm ch}/d\eta$ [43], p_T spectra [44], and $v_2(p_T)$ of pions, kaons, and protons [32,45] in Pb-Pb collisions at $\sqrt{s_{NN}} = 5.02$ TeV, is used for the longitudinal polarization calculation. In the scenario where the polarization is calculated for the Λ and $\bar{\Lambda}$ at the freeze-out using hyperon mass for the mass of the spin carrier, the effect of thermal vorticity dominates over the shear-induced polarization and total $P_{z,s2}$ shows a negative sign. However, considering the constituent strange quark as the spin carrier and the hyperons inheriting the spin polarization of the strange quark at hadronization, the effect of fluid shear prevails over thermal vorticity and generates the correct sign for resulting $P_{z,s2}$ as shown in Figs. 2–4. In both cases, the effect of hadronic scatterings on the hyperon spin polarization is not considered. Note that theoretical models, including the spin degrees of freedom consistently through all the stages of heavy-ion collisions, are not yet well developed [46,47]. Comparison of the experimental results with the two scenarios discussed here provides a qualitative idea about the possible consequences of the different assumptions used to estimate hyperon polarization from the velocity and temperature gradients generated by hydrodynamic or transport models [23].

In summary, the polarization of Λ and $\bar{\Lambda}$ hyperons along the beam direction has been measured in Pb-Pb collisions at $\sqrt{s_{NN}} = 5.02$ TeV using the ALICE detector at the LHC. The polarization exhibits a clear second harmonic sine modulation as expected due to elliptic flow. This is the first experimental evidence of a significant z component of the hyperon polarization due to elliptic flow-induced vorticity at the LHC. The $P_{z,s2}$ measured in Pb-Pb collisions at $\sqrt{s_{NN}} = 5.02$ TeV is of similar magnitude as the one measured by the STAR Collaboration in Au-Au collisions at $\sqrt{s_{NN}} = 200$ GeV. No significant dependence of $P_{z,s2}$ on the rapidity is observed. The sign of the $P_{z,s2}$ is positive at both RHIC and the LHC and in disagreement with hydrodynamic and AMPT models estimations accounting only for the thermal vorticity. The introduction of shear-induced polarization [22,23] along with additional assumptions on the hadronization temperature or mass of the spin carrier reproduces the experimentally observed positive $P_{z,s2}$ at RHIC and the LHC energies. These studies indicate that longitudinal polarization is sensitive to the hydrodynamic gradients as well as the dynamics of the spin degrees of freedom through the different stages of the evolution of the system created in heavy-ion collisions. For a quantitative data to model comparison, a detailed theoretical understanding of the quark spin polarization in the quark–gluon plasma (QGP), spin transfer at the hadronization, and the effect of hadronic scattering on the spin polarization are required. The upcoming run 3 at the LHC will provide much larger data samples for more differential and precision measurements of local and global hyperon polarization and provide further constraints to the models aiming to explain the vorticity and the particle polarization in heavy-ion collisions.

The ALICE Collaboration thanks all its engineers and technicians for their invaluable contributions to the construction of the experiment and the CERN accelerator teams for the outstanding performance of the LHC complex. The ALICE Collaboration gratefully acknowledges the resources and support provided by all Grid centers and the Worldwide LHC Computing Grid (WLCG) Collaboration. The ALICE Collaboration acknowledges the following funding agencies for their support in building and running the ALICE detector: A. I. Alikhanyan National Science Laboratory (Yerevan Physics Institute) Foundation (ANSL), State Committee of Science and World Federation of Scientists (WFS), Armenia; Austrian Academy of Sciences, Austrian Science Fund (FWF): [M 2467-N36] and Nationalstiftung für Forschung, Technologie und Entwicklung, Austria; Ministry of Communications and High Technologies, National Nuclear Research Center, Azerbaijan; Conselho Nacional de Desenvolvimento Científico e Tecnológico (CNPq), Financiadora de Estudos e Projetos (Finep), Fundação de Amparo à Pesquisa do Estado de São Paulo (FAPESP), and Universidade Federal do Rio Grande do Sul (UFRGS), Brazil; Ministry of Education of China (MOEC), Ministry of Science and Technology of China (MSTC), and National Natural Science Foundation of China (NSFC), China; Ministry of Science and Education and Croatian Science Foundation, Croatia; Centro de Aplicaciones Tecnológicas y Desarrollo Nuclear (CEADEN), Cubaenergía, Cuba; Ministry of Education, Youth and Sports of the Czech Republic, Czech Republic; The Danish Council for Independent Research | Natural Sciences, the VILLUM FONDEN, and Danish National Research Foundation

(DNRF), Denmark; Helsinki Institute of Physics (HIP), Finland; Commissariat à l'Energie Atomique (CEA) and Institut National de Physique Nucléaire et de Physique des Particules (IN2P3) and Centre National de la Recherche Scientifique (CNRS), France; Bundesministerium für Bildung und Forschung (BMBF) and GSI Helmholtzzentrum für Schwerionenforschung GmbH, Germany; General Secretariat for Research and Technology, Ministry of Education, Research and Religions, Greece; National Research, Development and Innovation Office, Hungary; Department of Atomic Energy Government of India (DAE), Department of Science and Technology, Government of India (DST), University Grants Commission, Government of India (UGC) and Council of Scientific and Industrial Research (CSIR), India; Indonesian Institute of Science, Indonesia; Istituto Nazionale di Fisica Nucleare (INFN), Italy; Institute for Innovative Science and Technology, Nagasaki Institute of Applied Science (IIST), Japanese Ministry of Education, Culture, Sports, Science and Technology (MEXT), and Japan Society for the Promotion of Science (JSPS) KAKENHI, Japan; Consejo Nacional de Ciencia (CONACYT) y Tecnología, through Fondo de Cooperación Internacional en Ciencia y Tecnología (FONCICYT) and Dirección General de Asuntos del Personal Academico (DGAPA), Mexico; Nederlandse Organisatie voor Wetenschappelijk Onderzoek (NWO), Netherlands; The Research Council of Norway, Norway; Commission on Science and Technology for Sustainable Development in the South (COMSATS), Pakistan; Pontificia Universidad Católica del Perú, Peru; Ministry of Education and Science, National Science Centre and WUT ID-UB, Poland; Korea Institute of Science and Technology Information and National Research Foundation of Korea (NRF), Republic of Korea; Ministry of Education and Scientific Research, Institute of Atomic Physics, and Ministry of Research and Innovation and Institute of Atomic Physics, Romania; Joint Institute for Nuclear Research (JINR), Ministry of Education and Science of the Russian Federation, National Research Centre Kurchatov Institute, Russian Science Foundation and Russian Foundation for Basic Research, Russia; Ministry of Education, Science, Research and Sport of the Slovak Republic, Slovakia; National Research Foundation of South Africa, South Africa; Swedish Research Council (VR) and Knut and Alice Wallenberg Foundation (KAW), Sweden; European Organization for Nuclear Research, Switzerland; Suranaree University of Technology (SUT), National Science and Technology Development Agency (NSDTA), and Office of the Higher Education Commission under NRU project of Thailand, Thailand; Turkish Energy, Nuclear and Mineral Research Agency (TENMAK), Turkey; National Academy of Sciences of Ukraine, Ukraine; Science and Technology Facilities Council (STFC), United Kingdom; National Science Foundation of the United States of America (NSF) and United States Department of Energy, Office of Nuclear Physics (DOE NP), United States of America.

[1] P. Braun-Munzinger, V. Koch, T. Schäfer, and J. Stachel, Properties of hot and dense matter from relativistic heavy ion collisions, Phys. Rep. **621**, 76 (2016).

[2] Z.-T. Liang and X.-N. Wang, Globally Polarized Quark-Gluon Plasma in Non-Central $A + A$ Collisions, Phys. Rev. Lett. **94**, 102301 (2005); **96**, 039901(E) (2006).

[3] S. A. Voloshin, Polarized secondary particles in unpolarized high energy hadron-hadron collisions?, arXiv:nucl-th/0410089.

[4] F. Becattini, G. Inghirami, V. Rolando, A. Beraudo, L. Del Zanna, A. De Pace, M. Nardi, G. Pagliara, and V. Chandra, A study of vorticity formation in high energy nuclear collisions, Eur. Phys. J. C **75**, 406 (2015); **78**, 354(E) (2018).

[5] L. Adamczyk *et al.* (STAR Collaboration), Global Λ hyperon polarization in nuclear collisions: Evidence for the most vortical fluid, Nature (London) **548**, 62 (2017).

[6] J. Adam *et al.* (STAR Collaboration), Global polarization of Λ hyperons in Au + Au collisions at $\sqrt{s_{NN}} = 200$ GeV, Phys. Rev. C **98**, 014910 (2018).

[7] S. Acharya *et al.* (ALICE Collaboration), Global polarization of $\Lambda\bar{\Lambda}$ hyperons in Pb-Pb collisions at $\sqrt{s_{NN}} = 2.76$ and 5.02 TeV, Phys. Rev. C **101**, 044611 (2020).

[8] S. A. Voloshin, Vorticity and particle polarization in heavy ion collisions (experimental perspective), EPJ Web Conf. **171**, 07002 (2018).

[9] B. Abelev *et al.* (ALICE Collaboration), Directed Flow of Charged Particles at Midrapidity Relative to the Spectator Plane in Pb-Pb Collisions at $\sqrt{s_{NN}} = 2.76$ TeV, Phys. Rev. Lett. **111**, 232302 (2013).

[10] H. Sorge, A. von Keitz, R. Mattiello, H. Stoecker, and W. Greiner, Baryon stopping, flow and equilibration in ultra-relativistic heavy ion collisions, Nucl. Phys. **A525**, 95C (1991).

[11] B. Betz, M. Gyulassy, and G. Torrieri, Polarization probes of vorticity in heavy ion collisions, Phys. Rev. C **76**, 044901 (2007).

[12] F. Becattini and I. Karpenko, Collective Longitudinal Polarization in Relativistic Heavy-Ion Collisions at Very High Energy, Phys. Rev. Lett. **120**, 012302 (2018).

[13] L.-G. Pang, H. Petersen, Q. Wang, and X.-N. Wang, Vortical Fluid and Λ Spin Correlations in High-Energy Heavy-Ion Collisions, Phys. Rev. Lett. **117**, 192301 (2016).

[14] X.-L. Xia, H. Li, Z.-B. Tang, and Q. Wang, Probing vorticity structure in heavy-ion collisions by local Λ polarization, Phys. Rev. C **98**, 024905 (2018).

[15] Y. Sun and C. M. Ko, Azimuthal angle dependence of the longitudinal spin polarization in relativistic heavy ion collisions, Phys. Rev. C **99**, 011903(R) (2019).

[16] J. Adam *et al.* (STAR Collaboration), Polarization of Λ ($\bar{\Lambda}$) Hyperons Along the Beam Direction in Au + Au Collisions at $\sqrt{s_{NN}} = 200$ GeV, Phys. Rev. Lett. **123**, 132301 (2019).

[17] B. Fu, K. Xu, X.-G. Huang, and H. Song, Hydrodynamic study of hyperon spin polarization in relativistic heavy ion collisions, Phys. Rev. C **103**, 024903 (2021).
[18] W. Florkowski, A. Kumar, A. Mazeliauskas, and R. Ryblewski, Longitudinal spin polarization in a thermal model, Phys. Rev. C **100**, 054907 (2019).
[19] X.-G. Huang, J. Liao, Q. Wang, and X.-L. Xia, Vorticity and spin polarization in heavy ion collisions: Transport models, arXiv:2010.08937.
[20] S. Y. F. Liu and Y. Yin, Spin polarization induced by the hydrodynamic gradients, J. High Energy Phys. 07 (2021) 188.
[21] F. Becattini, M. Buzzegoli, and A. Palermo, Spin-thermal shear coupling in a relativistic fluid, Phys. Lett. B **820**, 136519 (2021).
[22] F. Becattini, M. Buzzegoli, A. Palermo, G. Inghirami, and I. Karpenko, Local Polarization and Isothermal Local Equilibrium in Relativistic Heavy Ion Collisions, Phys. Rev. Lett. **127**, 272302 (2021).
[23] B. Fu, S. Y. F. Liu, L. Pang, H. Song, and Y. Yin, Shear-Induced Spin Polarization in Heavy-Ion Collisions, Phys. Rev. Lett. **127**, 142301 (2021).
[24] T. D. Lee and C.-N. Yang, General partial wave analysis of the decay of a hyperon of spin $1/2$, Phys. Rev. **108**, 1645 (1957).
[25] M. Ablikim *et al.* (BESIII Collaboration), Polarization and entanglement in baryon-antibaryon pair production in electron-positron annihilation, Nat. Phys. **15**, 631 (2019).
[26] K. Aamodt *et al.* (ALICE Collaboration), The ALICE experiment at the CERN LHC, J. Instrum. **3**, S08002 (2008).
[27] B. B. Abelev *et al.* (ALICE Collaboration), Performance of the ALICE experiment at the CERN LHC, Int. J. Mod. Phys. A **29**, 1430044 (2014).
[28] E. Abbas *et al.* (ALICE Collaboration), Performance of the ALICE VZERO system, J. Instrum. **8**, P10016 (2013).
[29] G. Dellacasa *et al.* (ALICE Collaboration), ALICE: Technical design report of the time projection chamber, Report Nos. CERN-OPEN-2000-183, CERN-LHCC-2000-001, 2000, https://cds.cern.ch/record/451098/.
[30] G. Dellacasa *et al.* (ALICE Collaboration), ALICE technical design report of the inner tracking system (ITS), Report No. CERN-LHCC-99-12, 1999, https://cds.cern.ch/record/391175/.
[31] P. A. Zyla *et al.* (Particle Data Group Collaboration), Review of particle physics, Prog. Theor. Exp. Phys. **2020**, 083C01 (2020).
[32] S. Acharya *et al.* (ALICE Collaboration), Anisotropic flow of identified particles in Pb-Pb collisions at $\sqrt{s_{\mathrm{NN}}} = 5.02$ TeV, J. High Energy Phys. 09 (2018) 006.
[33] A. M. Poskanzer and S. A. Voloshin, Methods for analyzing anisotropic flow in relativistic nuclear collisions, Phys. Rev. C **58**, 1671 (1998).
[34] F. Becattini, I. Karpenko, M. A. Lisa, I. Upsal, and S. A. Voloshin, Global hyperon polarization at local thermodynamic equilibrium with vorticity, magnetic field and feed-down, Phys. Rev. C **95**, 054902 (2017).
[35] X.-N. Wang and M. Gyulassy, HIJING: A Monte Carlo model for multiple jet production in p p, p A and A A collisions, Phys. Rev. D **44**, 3501 (1991).
[36] R. Brun, R. Hagelberg, M. Hansroul, and J. C. Lassalle, Simulation program for particle physics experiments, GEANT: User guide and reference manual, Reports No. CERN-DD-78-2-REV, CERN-DD-78-2, CERN, Geneva, 1978, https://cds.cern.ch/record/118715/.
[37] R. Barlow, Systematic errors: Facts and fictions, in *Conference on Advanced Statistical Techniques in Particle Physics* (University of Durham, Durham, 2002), https://arxiv.org/abs/hep-ex/0207026.
[38] B. Fu and H. Song (private communication), May 2021. For the description of the model see [23].
[39] B. Schenke, S. Jeon, and C. Gale, $(3+1)$D hydrodynamic simulation of relativistic heavy-ion collisions, Phys. Rev. C **82**, 014903 (2010).
[40] B. Schenke, S. Jeon, and C. Gale, Elliptic and Triangular Flow in Event-by-Event $(3+1)$D Viscous Hydrodynamics, Phys. Rev. Lett. **106**, 042301 (2011).
[41] Z.-W. Lin, C. M. Ko, B.-A. Li, B. Zhang, and S. Pal, A multi-phase transport model for relativistic heavy ion collisions, Phys. Rev. C **72**, 064901 (2005).
[42] H.-j. Xu, Z. Li, and H. Song, High-order flow harmonics of identified hadrons in 2.76A TeV Pb + Pb collisions, Phys. Rev. C **93**, 064905 (2016).
[43] J. Adam *et al.* (ALICE Collaboration), Centrality Dependence of the Charged-Particle Multiplicity Density at Mid-rapidity in Pb-Pb Collisions at $\sqrt{s_{\mathrm{NN}}} = 5.02$ TeV, Phys. Rev. Lett. **116**, 222302 (2016).
[44] S. Acharya *et al.* (ALICE Collaboration), Production of charged pions, kaons, and (anti-)protons in Pb-Pb and inelastic pp collisions at $\sqrt{s_{NN}} = 5.02$ TeV, Phys. Rev. C **101**, 044907 (2020).
[45] W. Zhao, H.-j. Xu, and H. Song, Collective flow in 2.76 A TeV and 5.02 A TeV Pb + Pb collisions, Eur. Phys. J. C **77**, 645 (2017).
[46] X.-L. Sheng, Q. Wang, and X.-N. Wang, Improved quark coalescence model for spin alignment and polarization of hadrons, Phys. Rev. D **102**, 056013 (2020).
[47] Z. Wang and P. Zhuang, Spin polarization induced by inhomogeneous dynamical condensate, arXiv:2101.00586.

S. Acharya,[143] D. Adamová,[98] A. Adler,[76] G. Aglieri Rinella,[35] M. Agnello,[31] N. Agrawal,[55] Z. Ahammed,[143] S. Ahmad,[16] S. U. Ahn,[78] I. Ahuja,[39] Z. Akbar,[52] A. Akindinov,[95] M. Al-Turany,[110] S. N. Alam,[16,41] D. Aleksandrov,[91] B. Alessandro,[61] H. M. Alfanda,[7] R. Alfaro Molina,[73] B. Ali,[16] Y. Ali,[14] A. Alici,[26a,26b] N. Alizadehvandchali,[127] A. Alkin,[35] J. Alme,[21] T. Alt,[70] L. Altenkamper,[21] I. Altsybeev,[115] M. N. Anaam,[7] C. Andrei,[49] D. Andreou,[93] A. Andronic,[146] M. Angeletti,[35] V. Anguelov,[107] F. Antinori,[58] P. Antonioli,[55] C. Anuj,[16] N. Apadula,[82] L. Aphecetche,[117] H. Appelshäuser,[70] S. Arcelli,[26a,26b] R. Arnaldi,[61] I. C. Arsene,[20] M. Arslandok,[107,148] A. Augustinus,[35] R. Averbeck,[110] S. Aziz,[80] M. D. Azmi,[16]

A. Badalà,[57] Y. W. Baek,[42] X. Bai,[110,131] R. Bailhache,[70] Y. Bailung,[51] R. Bala,[104] A. Balbino,[31] A. Baldisseri,[140] B. Balis,[2] M. Ball,[44] D. Banerjee,[4a,4b] R. Barbera,[27a,27b] L. Barioglio,[108] M. Barlou,[87] G. G. Barnaföldi,[147] L. S. Barnby,[97] V. Barret,[137] C. Bartels,[130] K. Barth,[35] E. Bartsch,[70] F. Baruffaldi,[28a,28b] N. Bastid,[137] S. Basu,[83] G. Batigne,[117] B. Batyunya,[77] D. Bauri,[50] J. L. Bazo Alba,[114] I. G. Bearden,[92] C. Beattie,[148] I. Belikov,[139] A. D. C. Bell Hechavarria,[146] F. Bellini,[26a,26b] R. Bellwied,[127] S. Belokurova,[115] V. Belyaev,[96] G. Bencedi,[71] S. Beole,[25a,25b] A. Bercuci,[49] Y. Berdnikov,[101] A. Berdnikova,[107] L. Bergmann,[107] M. G. Besoiu,[69] L. Betev,[35] P. P. Bhaduri,[143] A. Bhasin,[104] I. R. Bhat,[104] M. A. Bhat,[4a,4b] B. Bhattacharjee,[43] P. Bhattacharya,[23a,23b] L. Bianchi,[25a,25b] N. Bianchi,[53] J. Bielčík,[38] J. Bielčíková,[98] J. Biernat,[120] A. Bilandzic,[108] G. Biro,[147] S. Biswas,[4a,4b] J. T. Blair,[121] D. Blau,[84,91] M. B. Blidaru,[110] C. Blume,[70] G. Boca,[29,59] F. Bock,[99] A. Bogdanov,[96] S. Boi,[23a,23b] J. Bok,[63] L. Boldizsár,[147] A. Bolozdynya,[96] M. Bombara,[39] P. M. Bond,[35] G. Bonomi,[59,142] H. Borel,[140] A. Borissov,[84] H. Bossi,[148] E. Botta,[25a,25b] L. Bratrud,[70] P. Braun-Munzinger,[110] M. Bregant,[123] M. Broz,[38] G. E. Bruno,[34a,34b,109] M. D. Buckland,[130] D. Budnikov,[111] H. Buesching,[70] S. Bufalino,[31] O. Bugnon,[117] P. Buhler,[116] Z. Buthelezi,[74,134] J. B. Butt,[14] S. A. Bysiak,[120] M. Cai,[7,28a,28b] H. Caines,[148] A. Caliva,[110] E. Calvo Villar,[114] J. M. M. Camacho,[122] R. S. Camacho,[46] P. Camerini,[24a,24b] F. D. M. Canedo,[123] F. Carnesecchi,[26a,26b,35] R. Caron,[140] J. Castillo Castellanos,[140] E. A. R. Casula,[23a,23b] F. Catalano,[31] C. Ceballos Sanchez,[77] P. Chakraborty,[50] S. Chandra,[143] S. Chapeland,[35] M. Chartier,[130] S. Chattopadhyay,[143] S. Chattopadhyay,[112] A. Chauvin,[23a,23b] T. G. Chavez,[46] T. Cheng,[7] C. Cheshkov,[138] B. Cheynis,[138] V. Chibante Barroso,[35] D. D. Chinellato,[124] S. Cho,[63] P. Chochula,[35] P. Christakoglou,[93] C. H. Christensen,[92] P. Christiansen,[83] T. Chujo,[136] C. Cicalo,[56] L. Cifarelli,[26a,26b] F. Cindolo,[55] M. R. Ciupek,[110] G. Clai,[55,‡] J. Cleymans,[126,†] F. Colamaria,[54] J. S. Colburn,[113] D. Colella,[34a,34b,54,109,147] A. Collu,[82] M. Colocci,[35] M. Concas,[61,§] G. Conesa Balbastre,[81] Z. Conesa del Valle,[80] G. Contin,[24a,24b] J. G. Contreras,[38] M. L. Coquet,[140] T. M. Cormier,[99] P. Cortese,[32] M. R. Cosentino,[125] F. Costa,[35] S. Costanza,[29,59] P. Crochet,[137] R. Cruz-Torres,[82] E. Cuautle,[71] P. Cui,[7] L. Cunqueiro,[99] A. Dainese,[58] M. C. Danisch,[107] A. Danu,[69] I. Das,[112] P. Das,[89] P. Das,[4a,4b] S. Das,[4a,4b] S. Dash,[50] S. De,[89] A. De Caro,[30a,30b] G. de Cataldo,[54] L. De Cilladi,[25a,25b] J. de Cuveland,[40] A. De Falco,[23a,23b] D. De Gruttola,[30a,30b] N. De Marco,[61] C. De Martin,[24a,24b] S. De Pasquale,[30a,30b] S. Deb,[51] H. F. Degenhardt,[123] K. R. Deja,[144] L. Dello Stritto,[30a,30b] S. Delsanto,[25a,25b] W. Deng,[7] P. Dhankher,[19] D. Di Bari,[34a,34b] A. Di Mauro,[35] R. A. Diaz,[8] T. Dietel,[126] Y. Ding,[7,138] R. Divià,[35] D. U. Dixit,[19] Ø. Djuvsland,[21] U. Dmitrieva,[65] J. Do,[63] A. Dobrin,[69] B. Dönigus,[70] O. Dordic,[20] A. K. Dubey,[143] A. Dubla,[93,110] S. Dudi,[103] M. Dukhishyam,[89] P. Dupieux,[137] N. Dzalaiova,[13] T. M. Eder,[146] R. J. Ehlers,[99] V. N. Eikeland,[21] F. Eisenhut,[70] D. Elia,[54] B. Erazmus,[117] F. Ercolessi,[26a,26b] F. Erhardt,[102] A. Erokhin,[115] M. R. Ersdal,[21] B. Espagnon,[80] G. Eulisse,[35] D. Evans,[113] S. Evdokimov,[94] L. Fabbietti,[108] M. Faggin,[28a,28b] J. Faivre,[81] F. Fan,[7] A. Fantoni,[53] M. Fasel,[99] P. Fecchio,[31] A. Feliciello,[61] G. Feofilov,[115] A. Fernández Téllez,[46] A. Ferrero,[140] A. Ferretti,[25a,25b] V. J. G. Feuillard,[107] J. Figiel,[120] S. Filchagin,[111] D. Finogeev,[65] F. M. Fionda,[21,56] G. Fiorenza,[35,109] F. Flor,[127] A. N. Flores,[121] S. Foertsch,[74] P. Foka,[110] S. Fokin,[91] E. Fragiacomo,[62] E. Frajna,[147] U. Fuchs,[35] N. Funicello,[30a,30b] C. Furget,[81] A. Furs,[65] J. J. Gaardhøje,[92] M. Gagliardi,[25a,25b] A. M. Gago,[114] A. Gal,[139] C. D. Galvan,[122] P. Ganoti,[87] C. Garabatos,[110] J. R. A. Garcia,[46] E. Garcia-Solis,[10] K. Garg,[117] C. Gargiulo,[35] A. Garibli,[90] K. Garner,[146] P. Gasik,[110] E. F. Gauger,[121] A. Gautam,[129] M. B. Gay Ducati,[72] M. Germain,[117] P. Ghosh,[143] S. K. Ghosh,[4a,4b] M. Giacalone,[26a,26b] P. Gianotti,[53] P. Giubellino,[61,110] P. Giubilato,[28a,28b] A. M. C. Glaenzer,[140] P. Glässel,[107] D. J. Q. Goh,[85] V. Gonzalez,[145] L. H. González-Trueba,[73] S. Gorbunov,[40] M. Gorgon,[2] L. Görlich,[120] S. Gotovac,[36] V. Grabski,[73] L. K. Graczykowski,[144] L. Greiner,[82] A. Grelli,[64] C. Grigoras,[35] V. Grigoriev,[96] S. Grigoryan,[1,77] O. S. Groettvik,[21] F. Grosa,[35,61] J. F. Grosse-Oetringhaus,[35] R. Grosso,[110] G. G. Guardiano,[124] R. Guernane,[81] M. Guilbaud,[117] K. Gulbrandsen,[92] T. Gunji,[135] W. Guo,[7] A. Gupta,[104] R. Gupta,[104] S. P. Guzman,[46] L. Gyulai,[147] M. K. Habib,[110] C. Hadjidakis,[80] G. Halimoglu,[70] H. Hamagaki,[85] G. Hamar,[147] M. Hamid,[7] R. Hannigan,[121] M. R. Haque,[89,144] A. Harlenderova,[110] J. W. Harris,[148] A. Harton,[10] J. A. Hasenbichler,[35] H. Hassan,[99] D. Hatzifotiadou,[55] P. Hauer,[44] L. B. Havener,[148] S. Hayashi,[135] S. T. Heckel,[108] E. Hellbär,[110] H. Helstrup,[37] T. Herman,[38] E. G. Hernandez,[46] G. Herrera Corral,[9] F. Herrmann,[146] K. F. Hetland,[37] H. Hillemanns,[35] C. Hills,[130] B. Hippolyte,[139] B. Hofman,[64] B. Hohlweger,[93] J. Honermann,[146] G. H. Hong,[149] D. Horak,[38] S. Hornung,[110] A. Horzyk,[2] R. Hosokawa,[15] Y. Hou,[7] P. Hristov,[35] C. Hughes,[133] P. Huhn,[70] T. J. Humanic,[100] H. Hushnud,[112] L. A. Husova,[146] A. Hutson,[127] D. Hutter,[40] J. P. Iddon,[35,130] R. Ilkaev,[111] H. Ilyas,[14] M. Inaba,[136] G. M. Innocenti,[35] M. Ippolitov,[91] A. Isakov,[38,98] M. S. Islam,[112] M. Ivanov,[110] V. Ivanov,[101] V. Izucheev,[94] M. Jablonski,[2] B. Jacak,[82] N. Jacazio,[35] P. M. Jacobs,[82] S. Jadlovska,[119] J. Jadlovsky,[119] S. Jaelani,[64] C. Jahnke,[123,124] M. J. Jakubowska,[144] A. Jalotra,[104] M. A. Janik,[144] T. Janson,[76] M. Jercic,[102] O. Jevons,[113] A. A. P. Jimenez,[71] F. Jonas,[99,146] P. G. Jones,[113] J. M. Jowett,[35,110] J. Jung,[70] M. Jung,[70] A. Junique,[35] A. Jusko,[113]

J. Kaewjai,[118] P. Kalinak,[66] A. Kalweit,[35] V. Kaplin,[96] S. Kar,[7] A. Karasu Uysal,[79] D. Karatovic,[102] O. Karavichev,[65] T. Karavicheva,[65] P. Karczmarczyk,[144] E. Karpechev,[65] A. Kazantsev,[91] U. Kebschull,[76] R. Keidel,[48] D. L. D. Keijdener,[64] M. Keil,[35] B. Ketzer,[44] Z. Khabanova,[93] A. M. Khan,[7] S. Khan,[16] A. Khanzadeev,[101] Y. Kharlov,[84,94] A. Khatun,[16] A. Khuntia,[120] B. Kileng,[37] B. Kim,[17,63] C. Kim,[17] D. J. Kim,[128] E. J. Kim,[75] J. Kim,[149] J. S. Kim,[42] J. Kim,[107] J. Kim,[149] J. Kim,[75] M. Kim,[107] S. Kim,[18] T. Kim,[149] S. Kirsch,[70] I. Kisel,[40] S. Kiselev,[95] A. Kisiel,[144] J. P. Kitowski,[2] J. L. Klay,[6] J. Klein,[35] S. Klein,[82] C. Klein-Bösing,[146] M. Kleiner,[70] T. Klemenz,[108] A. Kluge,[35] A. G. Knospe,[127] C. Kobdaj,[118] M. K. Köhler,[107] T. Kollegger,[110] A. Kondratyev,[77] N. Kondratyeva,[96] E. Kondratyuk,[94] J. Konig,[70] S. A. Konigstorfer,[108] P. J. Konopka,[2,35] G. Kornakov,[144] S. D. Koryciak,[2] L. Koska,[119] A. Kotliarov,[98] O. Kovalenko,[88] V. Kovalenko,[115] M. Kowalski,[120] I. Králik,[66] A. Kravčáková,[39] L. Kreis,[110] M. Krivda,[66,113] F. Krizek,[98] K. Krizkova Gajdosova,[38] M. Kroesen,[107] M. Krüger,[70] E. Kryshen,[101] M. Krzewicki,[40] V. Kučera,[35] C. Kuhn,[139] P. G. Kuijer,[93] T. Kumaoka,[136] D. Kumar,[143] L. Kumar,[103] N. Kumar,[103] S. Kundu,[35,89] P. Kurashvili,[88] A. Kurepin,[65] A. B. Kurepin,[65] A. Kuryakin,[111] S. Kushpil,[98] J. Kvapil,[113] M. J. Kweon,[63] J. Y. Kwon,[63] Y. Kwon,[149] S. L. La Pointe,[40] P. La Rocca,[27a,27b] Y. S. Lai,[82] A. Lakrathok,[118] M. Lamanna,[35] R. Langoy,[132] K. Lapidus,[35] P. Larionov,[35,53] E. Laudi,[35] L. Lautner,[35,108] R. Lavicka,[38] T. Lazareva,[115] R. Lea,[24a,24b,59,142] J. Lehrbach,[40] R. C. Lemmon,[97] I. León Monzón,[122] E. D. Lesser,[19] M. Lettrich,[35,108] P. Lévai,[147] X. Li,[11] X. L. Li,[7] J. Lien,[132] R. Lietava,[113] B. Lim,[17] S. H. Lim,[17] V. Lindenstruth,[40] A. Lindner,[49] C. Lippmann,[110] A. Liu,[19] D. H. Liu,[7] J. Liu,[130] I. M. Lofnes,[21] V. Loginov,[96] C. Loizides,[99] P. Loncar,[36] J. A. Lopez,[107] X. Lopez,[137] E. López Torres,[8] J. R. Luhder,[146] M. Lunardon,[28a,28b] G. Luparello,[62] Y. G. Ma,[41] A. Maevskaya,[65] M. Mager,[35] T. Mahmoud,[44] A. Maire,[139] M. Malaev,[101] N. M. Malik,[104] Q. W. Malik,[20] L. Malinina,[77,‖] D. Mal'Kevich,[95] N. Mallick,[51] P. Malzacher,[110] G. Mandaglio,[33,57] V. Manko,[91] F. Manso,[137] V. Manzari,[54] Y. Mao,[7] J. Mareš,[68] G. V. Margagliotti,[24a,24b] A. Margotti,[55] A. Marín,[110] C. Markert,[121] M. Marquard,[70] N. A. Martin,[107] P. Martinengo,[35] J. L. Martinez,[127] M. I. Martínez,[46] G. Martínez García,[117] S. Masciocchi,[110] M. Masera,[25a,25b] A. Masoni,[56] L. Massacrier,[80] A. Mastroserio,[54,141] A. M. Mathis,[108] O. Matonoha,[83] P. F. T. Matuoka,[123] A. Matyja,[120] C. Mayer,[120] A. L. Mazuecos,[35] F. Mazzaschi,[25a,25b] M. Mazzilli,[35] M. A. Mazzoni,[60,†] J. E. Mdhluli,[134] A. F. Mechler,[70] F. Meddi,[22a,22b] Y. Melikyan,[65] A. Menchaca-Rocha,[73] E. Meninno,[30a,30b,116] A. S. Menon,[127] M. Meres,[13] S. Mhlanga,[74,126] Y. Miake,[136] L. Micheletti,[25a,25b,61] L. C. Migliorin,[138] D. L. Mihaylov,[108] K. Mikhaylov,[77,95] A. N. Mishra,[147] D. Miśkowiec,[110] A. Modak,[4a,4b] A. P. Mohanty,[64] B. Mohanty,[89] M. Mohisin Khan,[16,¶] M. A. Molander,[45] Z. Moravcova,[92] C. Mordasini,[108] D. A. Moreira De Godoy,[146] L. A. P. Moreno,[46] I. Morozov,[65] A. Morsch,[35] T. Mrnjavac,[35] V. Muccifora,[53] E. Mudnic,[36] D. Mühlheim,[146] S. Muhuri,[143] J. D. Mulligan,[82] A. Mulliri,[23a,23b] M. G. Munhoz,[123] R. H. Munzer,[70] H. Murakami,[135] S. Murray,[126] L. Musa,[35] J. Musinsky,[66] J. W. Myrcha,[144] B. Naik,[50,134] R. Nair,[88] B. K. Nandi,[50] R. Nania,[55] E. Nappi,[54] A. F. Nassirpour,[83] A. Nath,[107] C. Nattrass,[133] A. Neagu,[20] L. Nellen,[71] S. V. Nesbo,[37] G. Neskovic,[40] D. Nesterov,[115] B. S. Nielsen,[92] S. Nikolaev,[91] S. Nikulin,[91] V. Nikulin,[101] F. Noferini,[55] S. Noh,[12] P. Nomokonov,[77] J. Norman,[130] N. Novitzky,[136] P. Nowakowski,[144] A. Nyanin,[91] J. Nystrand,[21] M. Ogino,[85] A. Ohlson,[83] V. A. Okorokov,[96] J. Oleniacz,[144] A. C. Oliveira Da Silva,[133] M. H. Oliver,[148] A. Onnerstad,[128] C. Oppedisano,[61] A. Ortiz Velasquez,[71] T. Osako,[47] A. Oskarsson,[83] J. Otwinowski,[120] M. Oya,[47] K. Oyama,[85] Y. Pachmayer,[107] S. Padhan,[50] D. Pagano,[59,142] G. Paić,[71] A. Palasciano,[54] J. Pan,[145] S. Panebianco,[140] P. Pareek,[143] J. Park,[63] J. E. Parkkila,[128] S. P. Pathak,[127] R. N. Patra,[35,104] B. Paul,[23a,23b] H. Pei,[7] T. Peitzmann,[64] X. Peng,[7] L. G. Pereira,[72] H. Pereira Da Costa,[140] D. Peresunko,[84,91] G. M. Perez,[8] S. Perrin,[140] Y. Pestov,[5] V. Petráček,[38] M. Petrovici,[49] R. P. Pezzi,[72,117] S. Piano,[62] M. Pikna,[13] P. Pillot,[117] O. Pinazza,[35,55] L. Pinsky,[127] C. Pinto,[27a,27b] S. Pisano,[53] M. Płoskoń,[82] M. Planinic,[102] F. Pliquett,[70] M. G. Poghosyan,[99] B. Polichtchouk,[94] S. Politano,[31] N. Poljak,[102] A. Pop,[49] S. Porteboeuf-Houssais,[137] J. Porter,[82] V. Pozdniakov,[77] S. K. Prasad,[4a,4b] R. Preghenella,[55] F. Prino,[61] C. A. Pruneau,[145] I. Pshenichnov,[65] M. Puccio,[35] S. Qiu,[93] L. Quaglia,[25a,25b] R. E. Quishpe,[127] S. Ragoni,[113] A. Rakotozafindrabe,[140] L. Ramello,[32] F. Rami,[139] S. A. R. Ramirez,[46] A. G. T. Ramos,[34a,34b] T. A. Rancien,[81] R. Raniwala,[105] S. Raniwala,[105] S. S. Räsänen,[45] R. Rath,[51] I. Ravasenga,[93] K. F. Read,[99,133] A. R. Redelbach,[40] K. Redlich,[88,**] A. Rehman,[21] P. Reichelt,[70] F. Reidt,[35] H. A. Reme-ness,[37] R. Renfordt,[70] Z. Rescakova,[39] K. Reygers,[107] A. Riabov,[101] V. Riabov,[101] T. Richert,[83] M. Richter,[20] W. Riegler,[35] F. Riggi,[27a,27b] C. Ristea,[69] M. Rodríguez Cahuantzi,[46] K. Røed,[20] R. Rogalev,[94] E. Rogochaya,[77] T. S. Rogoschinski,[70] D. Rohr,[35] D. Röhrich,[21] P. F. Rojas,[46] P. S. Rokita,[144] F. Ronchetti,[53] A. Rosano,[33,57] E. D. Rosas,[71] A. Rossi,[58] A. Rotondi,[29,59] A. Roy,[51] P. Roy,[112] S. Roy,[50] N. Rubini,[26a,26b] O. V. Rueda,[83] R. Rui,[24a,24b] B. Rumyantsev,[77] P. G. Russek,[2] A. Rustamov,[90] E. Ryabinkin,[91] Y. Ryabov,[101] A. Rybicki,[120] H. Rytkonen,[128] W. Rzesa,[144] O. A. M. Saarimaki,[45] R. Sadek,[117] S. Sadovsky,[94] J. Saetre,[21] K. Šafařík,[38] S. K. Saha,[143] S. Saha,[89] B. Sahoo,[50] P. Sahoo,[50] R. Sahoo,[51] S. Sahoo,[67] D. Sahu,[51] P. K. Sahu,[67] J. Saini,[143] S. Sakai,[136] S. Sambyal,[104]

V. Samsonov,[96,101,†] D. Sarkar,[145] N. Sarkar,[143] P. Sarma,[43] V. M. Sarti,[108] M. H. P. Sas,[148] J. Schambach,[99,121] H. S. Scheid,[70] C. Schiaua,[49] R. Schicker,[107] A. Schmah,[107] C. Schmidt,[110] H. R. Schmidt,[106] M. O. Schmidt,[35] M. Schmidt,[106] N. V. Schmidt,[70,99] A. R. Schmier,[133] R. Schotter,[139] J. Schukraft,[35] Y. Schutz,[139] K. Schwarz,[110] K. Schweda,[110] G. Scioli,[26a,26b] E. Scomparin,[61] J. E. Seger,[15] Y. Sekiguchi,[135] D. Sekihata,[135] I. Selyuzhenkov,[96,110] S. Senyukov,[139] J. J. Seo,[63] D. Serebryakov,[65] L. Šerkšnytė,[108] A. Sevcenco,[69] T. J. Shaba,[74] A. Shabanov,[65] A. Shabetai,[117] R. Shahoyan,[35] W. Shaikh,[112] A. Shangaraev,[94] A. Sharma,[103] H. Sharma,[120] M. Sharma,[104] N. Sharma,[103] S. Sharma,[104] U. Sharma,[104] O. Sheibani,[127] K. Shigaki,[47] M. Shimomura,[86] S. Shirinkin,[95] Q. Shou,[41] Y. Sibiriak,[91] S. Siddhanta,[56] T. Siemiarczuk,[88] T. F. Silva,[123] D. Silvermyr,[83] T. Simantathammakul,[118] G. Simonetti,[35] B. Singh,[108] R. Singh,[89] R. Singh,[104] R. Singh,[51] V. K. Singh,[143] V. Singhal,[143] T. Sinha,[112] B. Sitar,[13] M. Sitta,[32] T. B. Skaali,[20] G. Skorodumovs,[107] M. Slupecki,[45] N. Smirnov,[148] R. J. M. Snellings,[64] C. Soncco,[114] J. Song,[127] A. Songmoolnak,[118] F. Soramel,[28a,28b] S. Sorensen,[133] I. Sputowska,[120] J. Stachel,[107] I. Stan,[69] P. J. Steffanic,[133] S. F. Stiefelmaier,[107] D. Stocco,[117] I. Storehaug,[20] M. M. Storetvedt,[37] C. P. Stylianidis,[93] A. A. P. Suaide,[123] T. Sugitate,[47] C. Suire,[80] M. Sukhanov,[65] M. Suljic,[35] R. Sultanov,[95] M. Šumbera,[98] V. Sumberia,[104] S. Sumowidagdo,[52] S. Swain,[67] A. Szabo,[13] I. Szarka,[13] U. Tabassam,[14] S. F. Taghavi,[108] G. Taillepied,[137] J. Takahashi,[124] G. J. Tambave,[21] S. Tang,[7,137] Z. Tang,[131] J. D. Tapia Takaki,[129,†,†] M. Tarhini,[117] M. G. Tarzila,[49] A. Tauro,[35] G. Tejeda Muñoz,[46] A. Telesca,[35] L. Terlizzi,[25a,25b] C. Terrevoli,[127] G. Tersimonov,[3] S. Thakur,[143] D. Thomas,[121] R. Tieulent,[138] A. Tikhonov,[65] A. R. Timmins,[127] M. Tkacik,[119] A. Toia,[70] N. Topilskaya,[65] M. Toppi,[53] F. Torales-Acosta,[19] T. Tork,[80] S. R. Torres,[38] A. Trifiró,[33,57] S. Tripathy,[55,71] T. Tripathy,[50] S. Trogolo,[28a,28b,35] G. Trombetta,[34a,34b] V. Trubnikov,[3] W. H. Trzaska,[128] T. P. Trzcinski,[144] B. A. Trzeciak,[38] A. Tumkin,[111] R. Turrisi,[58] T. S. Tveter,[20] K. Ullaland,[21] A. Uras,[138] M. Urioni,[59,142] G. L. Usai,[23a,23b] M. Vala,[39] N. Valle,[29,59] S. Vallero,[61] N. van der Kolk,[64] L. V. R. van Doremalen,[64] M. van Leeuwen,[93] P. Vande Vyvre,[35] D. Varga,[147] Z. Varga,[147] M. Varga-Kofarago,[147] A. Vargas,[46] M. Vasileiou,[87] A. Vasiliev,[91] O. Vázquez Doce,[53,108] V. Vechernin,[115] E. Vercellin,[25a,25b] S. Vergara Limón,[46] L. Vermunt,[64] R. Vértesi,[147] M. Verweij,[64] L. Vickovic,[36] Z. Vilakazi,[134] O. Villalobos Baillie,[113] G. Vino,[54] A. Vinogradov,[91] T. Virgili,[30a,30b] V. Vislavicius,[92] A. Vodopyanov,[77] B. Volkel,[35] M. A. Völkl,[107] K. Voloshin,[95] S. A. Voloshin,[145] G. Volpe,[34a,34b] B. von Haller,[35] I. Vorobyev,[108] D. Voscek,[119] N. Vozniuk,[65] J. Vrláková,[39] B. Wagner,[21] C. Wang,[41] D. Wang,[41] M. Weber,[116] R. J. G. V. Weelden,[93] A. Wegrzynek,[35] S. C. Wenzel,[35] J. P. Wessels,[146] J. Wiechula,[70] J. Wikne,[20] G. Wilk,[88] J. Wilkinson,[110] G. A. Willems,[146] B. Windelband,[107] M. Winn,[140] W. E. Witt,[133] J. R. Wright,[121] W. Wu,[41] Y. Wu,[131] R. Xu,[7] A. K. Yadav,[143] S. Yalcin,[79] Y. Yamaguchi,[47] K. Yamakawa,[47] S. Yang,[21] S. Yano,[47] Z. Yin,[7] H. Yokoyama,[64] I.-K. Yoo,[17] J. H. Yoon,[63] S. Yuan,[21] A. Yuncu,[107] V. Zaccolo,[24a,24b] C. Zampolli,[35] H. J. C. Zanoli,[64] N. Zardoshti,[35] A. Zarochentsev,[115] P. Závada,[68] N. Zaviyalov,[111] M. Zhalov,[101] B. Zhang,[7] S. Zhang,[41] X. Zhang,[7] Y. Zhang,[131] V. Zherebchevskii,[115] Y. Zhi,[11] N. Zhigareva,[95] D. Zhou,[7] Y. Zhou,[92] J. Zhu,[7,110] Y. Zhu,[7] A. Zichichi,[26a,26b] G. Zinovjev,[3] and N. Zurlo[142,59]

(ALICE Collaboration)

[1]*A.I. Alikhanyan National Science Laboratory (Yerevan Physics Institute) Foundation, Yerevan, Armenia*
[2]*AGH University of Science and Technology, Cracow, Poland*
[3]*Bogolyubov Institute for Theoretical Physics, National Academy of Sciences of Ukraine, Kiev, Ukraine*
[4a]*Bose Institute, Department of Physics, Kolkata, India*
[4b]*Centre for Astroparticle Physics and Space Science (CAPSS), Kolkata, India*
[5]*Budker Institute for Nuclear Physics, Novosibirsk, Russia*
[6]*California Polytechnic State University, San Luis Obispo, California, USA*
[7]*Central China Normal University, Wuhan, China*
[8]*Centro de Aplicaciones Tecnológicas y Desarrollo Nuclear (CEADEN), Havana, Cuba*
[9]*Centro de Investigación y de Estudios Avanzados (CINVESTAV), Mexico City and Mérida, Mexico*
[10]*Chicago State University, Chicago, Illinois, USA*
[11]*China Institute of Atomic Energy, Beijing, China*
[12]*Chungbuk National University, Cheongju, Republic of Korea*
[13]*Comenius University Bratislava, Faculty of Mathematics, Physics and Informatics, Bratislava, Slovakia*
[14]*COMSATS University Islamabad, Islamabad, Pakistan*
[15]*Creighton University, Nebraska, USA*
[16]*Department of Physics, Aligarh Muslim University, Aligarh, India*

[17]Department of Physics, Pusan National University, Pusan, Republic of Korea
[18]Department of Physics, Sejong University, Seoul, Republic of Korea
[19]Department of Physics, University of California, Berkeley, California, USA
[20]Department of Physics, University of Oslo, Oslo, Norway
[21]Department of Physics and Technology, University of Bergen, Bergen, Norway
[22a]Dipartimento di Fisica dell'Università "La Sapienza", Rome, Italy
[22b]Sezione INFN, Rome, Italy
[23a]Dipartimento di Fisica dell'Università, Cagliari, Italy
[23b]Sezione INFN, Cagliari, Italy
[24a]Dipartimento di Fisica dell'Università, Trieste, Italy
[24b]Sezione INFN, Trieste, Italy
[25a]Dipartimento di Fisica dell'Università, Turin, Italy
[25b]Sezione INFN, Turin, Italy
[26a]Dipartimento di Fisica e Astronomia dell'Università, Bologna, Italy
[26b]Sezione INFN, Bologna, Italy
[27a]Dipartimento di Fisica e Astronomia dell'Università, Catania, Italy
[27b]Sezione INFN, Catania, Italy
[28a]Dipartimento di Fisica e Astronomia dell'Università, Padova, Italy
[28b]Sezione INFN, Padova, Italy
[29]Dipartimento di Fisica e Nucleare e Teorica, Università di Pavia, Pavia, Italy
[30a]Dipartimento di Fisica "E.R. Caianiello" dell'Università, Salerno, Italy
[30b]Gruppo Collegato INFN, Salerno, Italy
[31]Dipartimento DISAT del Politecnico and Sezione INFN, Turin, Italy
[32]Dipartimento di Scienze e Innovazione Tecnologica dell'Università del Piemonte Orientale and INFN Sezione di Torino, Alessandria, Italy
[33]Dipartimento di Scienze MIFT, Università di Messina, Messina, Italy
[34a]Dipartimento Interateneo di Fisica "M. Merlin", Bari, Italy
[34b]Sezione INFN, Bari, Italy
[35]European Organization for Nuclear Research (CERN), Geneva, Switzerland
[36]Faculty of Electrical Engineering, Mechanical Engineering and Naval Architecture, University of Split, Split, Croatia
[37]Faculty of Engineering and Science, Western Norway University of Applied Sciences, Bergen, Norway
[38]Faculty of Nuclear Sciences and Physical Engineering, Czech Technical University in Prague, Prague, Czech Republic
[39]Faculty of Science, P.J. Šafárik University, Košice, Slovakia
[40]Frankfurt Institute for Advanced Studies, Johann Wolfgang Goethe-Universität Frankfurt, Frankfurt, Germany
[41]Fudan University, China
[42]Gangneung-Wonju National University, Gangneung, Republic of Korea
[43]Gauhati University, Department of Physics, Guwahati, India
[44]Helmholtz-Institut für Strahlen- und Kernphysik, Rheinische Friedrich-Wilhelms-Universität Bonn, Bonn, Germany
[45]Helsinki Institute of Physics (HIP), Helsinki, Finland
[46]High Energy Physics Group, Universidad Autónoma de Puebla, Puebla, Mexico
[47]Hiroshima University, Hiroshima, Japan
[48]Hochschule Worms, Zentrum für Technologietransfer und Telekommunikation (ZTT), Worms, Germany
[49]Horia Hulubei National Institute of Physics and Nuclear Engineering, Bucharest, Romania
[50]Indian Institute of Technology Bombay (IIT), Mumbai, India
[51]Indian Institute of Technology Indore, Indore, India
[52]Indonesian Institute of Sciences, Jakarta, Indonesia
[53]INFN, Laboratori Nazionali di Frascati, Frascati, Italy
[54]INFN, Sezione di Bari, Bari, Italy
[55]INFN, Sezione di Bologna, Bologna, Italy
[56]INFN, Sezione di Cagliari, Cagliari, Italy
[57]INFN, Sezione di Catania, Catania, Italy
[58]INFN, Sezione di Padova, Padova, Italy
[59]INFN, Sezione di Pavia, Pavia, Italy
[60]INFN, Sezione di Roma, Rome, Italy
[61]INFN, Sezione di Torino, Turin, Italy
[62]INFN, Sezione di Trieste, Trieste, Italy
[63]Inha University, Incheon, Republic of Korea
[64]Institute for Gravitational and Subatomic Physics (GRASP), Utrecht University/Nikhef, Utrecht, Netherlands
[65]Institute for Nuclear Research, Academy of Sciences, Moscow, Russia
[66]Institute of Experimental Physics, Slovak Academy of Sciences, Košice, Slovakia

[67]Institute of Physics, Homi Bhabha National Institute, Bhubaneswar, India
[68]Institute of Physics of the Czech Academy of Sciences, Prague, Czech Republic
[69]Institute of Space Science (ISS), Bucharest, Romania
[70]Institut für Kernphysik, Johann Wolfgang Goethe-Universität Frankfurt, Frankfurt, Germany
[71]Instituto de Ciencias Nucleares, Universidad Nacional Autónoma de México, Mexico City, Mexico
[72]Instituto de Física, Universidade Federal do Rio Grande do Sul (UFRGS), Porto Alegre, Brazil
[73]Instituto de Física, Universidad Nacional Autónoma de México, Mexico City, Mexico
[74]iThemba LABS, National Research Foundation, Somerset West, South Africa
[75]Jeonbuk National University, Jeonju, Republic of Korea
[76]Johann-Wolfgang-Goethe Universität Frankfurt Institut für Informatik, Fachbereich Informatik und Mathematik, Frankfurt, Germany
[77]Joint Institute for Nuclear Research (JINR), Dubna, Russia
[78]Korea Institute of Science and Technology Information, Daejeon, Republic of Korea
[79]KTO Karatay University, Konya, Turkey
[80]Laboratoire de Physique des 2 Infinis, Irène Joliot-Curie, Orsay, France
[81]Laboratoire de Physique Subatomique et de Cosmologie, Université Grenoble-Alpes, CNRS-IN2P3, Grenoble, France
[82]Lawrence Berkeley National Laboratory, Berkeley, California, USA
[83]Lund University Department of Physics, Division of Particle Physics, Division of Particle Physics, Lund, Sweden
[84]Moscow Institute for Physics and Technology, Moscow, Russia
[85]Nagasaki Institute of Applied Science, Nagasaki, Japan
[86]Nara Women's University (NWU), Nara, Japan
[87]National and Kapodistrian University of Athens, School of Science, Department of Physics, Athens, Greece
[88]National Centre for Nuclear Research, Warsaw, Poland
[89]National Institute of Science Education and Research, Homi Bhabha National Institute, Jatni, India
[90]National Nuclear Research Center, Baku, Azerbaijan
[91]National Research Centre Kurchatov Institute, Moscow, Russia
[92]Niels Bohr Institute, University of Copenhagen, Copenhagen, Denmark
[93]Nikhef, National institute for subatomic physics, Amsterdam, Netherlands
[94]NRC Kurchatov Institute IHEP, Protvino, Russia
[95]NRC «Kurchatov» Institute - ITEP, Moscow, Russia
[96]NRNU Moscow Engineering Physics Institute, Moscow, Russia
[97]Nuclear Physics Group, STFC Daresbury Laboratory, Daresbury, United Kingdom
[98]Nuclear Physics Institute of the Czech Academy of Sciences, Řež u Prahy, Czech Republic
[99]Oak Ridge National Laboratory, Oak Ridge, Tennessee, USA
[100]Ohio State University, Columbus, Ohio, USA
[101]Petersburg Nuclear Physics Institute, Gatchina, Russia
[102]Physics department, Faculty of science, University of Zagreb, Zagreb, Croatia
[103]Physics Department, Panjab University, Chandigarh, India
[104]Physics Department, University of Jammu, Jammu, India
[105]Physics Department, University of Rajasthan, Jaipur, India
[106]Physikalisches Institut, Eberhard-Karls-Universität Tübingen, Tübingen, Germany
[107]Physikalisches Institut, Ruprecht-Karls-Universität Heidelberg, Heidelberg, Germany
[108]Physik Department, Technische Universität München, Munich, Germany
[109]Politecnico di Bariand Sezione INFN, Bari, Italy
[110]Research Division and ExtreMe Matter Institute EMMI, GSI Helmholtzzentrum für Schwerionenforschung GmbH, Darmstadt, Germany
[111]Russian Federal Nuclear Center (VNIIEF), Sarov, Russia
[112]Saha Institute of Nuclear Physics, Homi Bhabha National Institute, Kolkata, India
[113]School of Physics and Astronomy, University of Birmingham, Birmingham, United Kingdom
[114]Sección Física, Departamento de Ciencias, Pontificia Universidad Católica del Perú, Lima, Peru
[115]St. Petersburg State University, St. Petersburg, Russia
[116]Stefan Meyer Institut für Subatomare Physik (SMI), Vienna, Austria
[117]SUBATECH, IMT Atlantique, Université de Nantes, CNRS-IN2P3, Nantes, France
[118]Suranaree University of Technology, Nakhon Ratchasima, Thailand
[119]Technical University of Košice, Košice, Slovakia
[120]The Henryk Niewodniczanski Institute of Nuclear Physics, Polish Academy of Sciences, Cracow, Poland
[121]The University of Texas at Austin, Austin, Texas, USA
[122]Universidad Autónoma de Sinaloa, Culiacán, Mexico
[123]Universidade de São Paulo (USP), São Paulo, Brazil
[124]Universidade Estadual de Campinas (UNICAMP), Campinas, Brazil

[125]Universidade Federal do ABC, Santo Andre, Brazil
[126]University of Cape Town, Cape Town, South Africa
[127]University of Houston, Houston, Texas, USA
[128]University of Jyväskylä, Jyväskylä, Finland
[129]University of Kansas, Lawrence, Kansas, USA
[130]University of Liverpool, Liverpool, United Kingdom
[131]University of Science and Technology of China, Hefei, China
[132]University of South-Eastern Norway, Tonsberg, Norway
[133]University of Tennessee, Knoxville, Tennessee, USA
[134]University of the Witwatersrand, Johannesburg, South Africa
[135]University of Tokyo, Tokyo, Japan
[136]University of Tsukuba, Tsukuba, Japan
[137]Université Clermont Auvergne, CNRS/IN2P3, LPC, Clermont-Ferrand, France
[138]Université de Lyon, CNRS/IN2P3, Institut de Physique des 2 Infinis de Lyon, Lyon, France
[139]Université de Strasbourg, CNRS, IPHC UMR 7178, F-67000 Strasbourg, France, Strasbourg, France
[140]Université Paris-Saclay Centre d'Etudes de Saclay (CEA), IRFU, Département de Physique Nucléaire (DPhN), Saclay, France
[141]Università degli Studi di Foggia, Foggia, Italy
[142]Università di Brescia, Brescia, Italy
[143]Variable Energy Cyclotron Centre, Homi Bhabha National Institute, Kolkata, India
[144]Warsaw University of Technology, Warsaw, Poland
[145]Wayne State University, Detroit, Michigan, USA
[146]Westfälische Wilhelms-Universität Münster, Institut für Kernphysik, Münster, Germany
[147]Wigner Research Centre for Physics, Budapest, Hungary
[148]Yale University, New Haven, Connecticut, USA
[149]Yonsei University, Seoul, Republic of Korea

[†]Deceased.
[‡]Also at Italian National Agency for New Technologies, Energy and Sustainable Economic Development (ENEA), Bologna, Italy.
[§]Also at Dipartimento DET del Politecnico di Torino, Turin, Italy.
[‖]Also at M.V. Lomonosov Moscow State University, D.V. Skobeltsyn Institute of Nuclear, Physics, Moscow, Russia.
[¶]Also at Department of Applied Physics, Aligarh Muslim University, Aligarh, India.
[**]Also at Institute of Theoretical Physics, University of Wroclaw, Poland.
[††]Also at University of Kansas, Lawrence, Kansas, USA.